Guo-Xiao Wang,[1,2] Kae Won Cho,[3,4] Maeran Uhm,[1,3,5] Chun-Rui Hu,[6] Siming Li,[1,2] Zoharit Cozacov,[1,2] Acer E. Xu,[1,2] Ji-Xin Cheng,[6] Alan R. Saltiel,[1,3,5] Carey N. Lumeng,[3,4] and Jiandie D. Lin[1,2]

Otopetrin 1 Protects Mice From Obesity-Associated Metabolic Dysfunction Through Attenuating Adipose Tissue Inflammation

PATHOPHYSIOLOGY

Chronic low-grade inflammation is emerging as a pathogenic link between obesity and metabolic disease. Persistent immune activation in white adipose tissue (WAT) impairs insulin sensitivity and systemic metabolism, in part, through the actions of proinflammatory cytokines. Whether obesity engages an adaptive mechanism to counteract chronic inflammation in adipose tissues has not been elucidated. Here we identified otopetrin 1 (Otop1) as a component of a counterinflammatory pathway that is induced in WAT during obesity. Otop1 expression is markedly increased in obese mouse WAT and is stimulated by tumor necrosis factor-α in cultured adipocytes. Otop1 mutant mice respond to high-fat diet with pronounced insulin resistance and hepatic steatosis, accompanied by augmented adipose tissue inflammation. Otop1 attenuates interferon-γ (IFN-γ) signaling in adipocytes through selective downregulation of the transcription factor STAT1. Using a tagged vector, we found that Otop1 physically interacts with endogenous STAT1. Thus, Otop1 defines a unique target of cytokine signaling that attenuates obesity-induced adipose tissue inflammation and plays an adaptive role in maintaining metabolic homeostasis in obesity.

Diabetes 2014;63:1340–1352 | DOI: 10.2337/db13-1139

Obesity poses significant risk to patient health owing to its associated metabolic disorders. White adipose tissue (WAT) stores the bulk of body fat and also plays an important role in endocrine metabolic signaling (1,2), whereas brown adipose tissue (BAT) defends against cold and obesity through uncoupled mitochondrial respiration (3,4). Obesity is associated with chronic low-grade inflammation in adipose tissues (5–9). The pathogenic role of the persistent activation of inflammatory signaling in metabolic disease has been demonstrated in numerous mouse models. An emerging view suggests that attenuating the proinflammatory response may provide significant metabolic benefits in obesity. While therapeutic development targeting inflammation remains in its early stage in humans, several candidates have shown promise, including salsalate, a prodrug of salicylate (10), and interleukin (IL)-1 receptor antagonists (11). In addition,

[1]Life Sciences Institute, University of Michigan Medical School, Ann Arbor, MI
[2]Department of Cell and Developmental Biology, University of Michigan Medical School, Ann Arbor, MI
[3]Department of Molecular and Integrative Physiology, University of Michigan Medical School, Ann Arbor, MI
[4]Department of Pediatrics and Communicable Diseases, University of Michigan Medical School, Ann Arbor, MI
[5]Department of Internal Medicine, University of Michigan Medical School, Ann Arbor, MI
[6]Weldon School of Biomedical Engineering, Department of Chemistry, Purdue University, West Lafayette, IN
Corresponding author: Jiandie D. Lin, jdlin@umich.edu.

Received 23 July 2013 and accepted 19 December 2013.
This article contains Supplementary Data online at http://diabetes.diabetesjournals.org/lookup/suppl/doi:10.2337/db13-1139/-/DC1.

the beneficial effects of peroxisome proliferator–activated receptor (PPAR)-γ agonists have, at least in part, been attributed to their anti-inflammatory activities (12,13).

The molecular and cellular events that lead to the engagement and sustained activation of the innate immune system in obesity are complex and remain to be unraveled. In adipose tissues, obesity-induced inflammation is associated with a robust shift of adipose tissue macrophages from alternatively activated (M2) to classically activated (M1) subtypes (14,15). This shift toward proinflammatory macrophage polarization coincides with the development of insulin resistance and has been proposed as an early event underlying metabolic dysregulation (16). A parallel shift from anti-inflammatory regulatory T cells to CD4+ helper and CD8+ cytotoxic T cells also occurs in WAT during obesity (17–19). The latter produces proinflammatory cytokines such as tumor necrosis factor-α (TNF-α), a prototypical cytokine associated with obesity (20), and interferon-γ (IFN-γ), which contribute to chronic inflammation in adipose tissues. Several pathways downstream of cytokine receptors have been shown to play a role in obesity-induced inflammation and its metabolic consequences, including inhibitor of nuclear factor κB kinase-β (IKK-β), nuclear factor-κB (NFκB), c-Jun NH_2-terminal kinase, IKK-ε, and inflammasome activation (21–26). The activation of these signaling pathways impairs insulin signaling in adipocytes. As such, genetic and pharmacological inhibition of these pathways leads to attenuation of inflammatory signaling and improved insulin sensitivity.

Multiple proinflammatory cytokines have been implicated in obesity-induced inflammation and contribute to the development of insulin resistance (1,27). While it is unlikely that the actions of any single cytokine could account for the complex and reciprocal interactions between immune cells and adipocytes, IFN-γ has emerged as a uniquely important cytokine in this context. IFN-γ transduces signals through the JAK/STAT pathway (28), particularly transcription factor STAT-1, and has been demonstrated to attenuate insulin signaling and lipid metabolism in adipocytes (29). Notably, mice lacking IFN-γ have reduced adipose tissue inflammation and improved metabolic homeostasis (30), suggesting that IFN-γ signaling is a key player that sustains a proinflammatory state in obesity. Despite a plethora of evidence supporting the pathogenic role of chronic inflammation, whether obesity activates adaptive pathways that counteract inflammation and the extent to which they contribute to metabolic homeostasis remain largely unknown.

Otopetrin 1 (Otop1) is a member of the otopetrin domain protein family that is highly conserved in species ranging from nematodes to vertebrates (31,32). Otop1 is predicted to contain 12 transmembrane domains and has been demonstrated to localize to the plasma membrane (33). Mice harboring *tilted* mutation (A151E, Otop1^{tlt}) have impaired otoconia development (34), likely as a consequence of altered cellular calcium in vestibular supporting cells (33,35). Importantly, Otop1 knockout mice develop similar defects in otoconia formation (36), suggesting that Otop1^{tlt} mutant represents a bona fide loss-of-function allele. Whether Otop1 is expressed in peripheral tissues and regulates other physiological processes remains unknown. In this study, we found that Otop1 is induced in WAT during obesity and counteracts obesity-associated adipose tissue inflammation. Otop1 defines a novel adaptive mechanism that maintains metabolic homeostasis through attenuating chronic inflammation.

RESEARCH DESIGN AND METHODS

Animals and Animal Care

All animal studies were performed following the guideline established by the University Committee on Use and Care of Animals at the University of Michigan. Mice were housed in a specific pathogen-free facility at 77°F with a 12-h light, 12-h dark cycle and free access to food and water. For chow diet feeding, male wild-type (WT) C57BL/6J mice and Otop1^{tlt} mice were fed with Teklad 5001 laboratory diet. For high-fat diet (HFD) feeding, mice were fed with a diet consisting of 60% of calories from fat (D12492, Research Diets Inc.) starting at 10 to 12 weeks of age.

Adipocyte Isolation and Differentiation

Immortalization and differentiation of brown adipocytes were performed as described (37). Briefly, SV40 large T antigen-immortalized brown preadipocytes were cultured in Dulbecco's modified Eagle's medium (DMEM) with 10% FBS. Differentiation was induced 2 days postconfluence (day 0) by adding a cocktail containing 0.5 mmol/L 3-isobutyl-1-methylxanthine, 125 μmol/L indomethacin, and 1 μmol/L dexamethasone to the maintenance media (DMEM supplemented with 10% FBS, 20 nmol/L insulin, and 1 nmol/L T3). Two days after induction, cells were cultured in the maintenance media alone. Total RNA was isolated at different days for gene expression analysis.

3T3-L1 fibroblasts were cultured in DMEM with 10% bovine growth serum until 2 days postconfluent. Differentiation was induced by adding a cocktail containing 0.5 mmol/L 3-isobutyl-1-methylxanthine, 1 μmol/L dexamethasone, and 1 μg/mL insulin to DMEM supplemented with 10% FBS. Three days after induction, cells were cultured in DMEM containing 10% FBS plus 1 μg/mL of insulin for 2 more days followed by maintenance in DMEM supplemented with 10% FBS. TNF-α, IFN-γ, and lipopolysaccharide (LPS) treatments were carried out in mature adipocytes cultured in the maintenance media.

Adipose Tissue Explant Culture

Epididymal WAT (eWAT) was dissected and transferred to a petri dish with 20 mL DMEM, cut into pieces with diameters less than 4 mm (~5–10 mg). Tissue pieces were filtered through 200 μm nylon mesh, washed once with 10× volume PBS and then with 10× volume DMEM, transferred into six-well plates with serum-free M199 media (1 nmol/L insulin, 1 nmol/L dexamethasone), and

cultured for 2 h before IFN-γ treatment at 10 ng/mL for 4 h. Following treatments, fat tissues were quickly dried on paper towels and processed for RNA isolation and quantitative real-time PCR (qPCR) gene expression analysis.

Metabolic and Gene Expression Analyses

Plasma concentrations of free glycerol and triglycerides (Sigma), β-hydroxybutyrate (Stanbio Laboratory), and nonesterified fatty acid (Wako Diagnostics) were measured using commercial assay kits. Liver triglyceride was extracted and measured as previously described (38). Plasma insulin was measured using an ELISA kit (CrystalChem). Glucose and insulin tolerance tests were performed as previously described (39). For insulin signaling studies, mice were fed HFD for 8 weeks before receiving a single dose of intravenous injection of saline or insulin (1.5 units/kg). Tissues were rapidly dissected 10 min after injection for immunoblotting analyses.

For gene expression analysis, total RNA from WAT was extracted using a commercial kit from Invitrogen. Total RNA from other tissues and cultured cells was extracted using the TRIzol method. For qPCR analysis, equal amount of RNA was reverse-transcribed using Moloney murine leukemia virus reverse transcriptase followed by qPCR reactions using SYBR Green (Life Technologies). Relative abundance of mRNA was normalized to ribosomal protein 36B4. Adipose tissue and liver gene expression was analyzed using specific primers (Supplementary Table 1). Statistical significance was determined by Student *t* test.

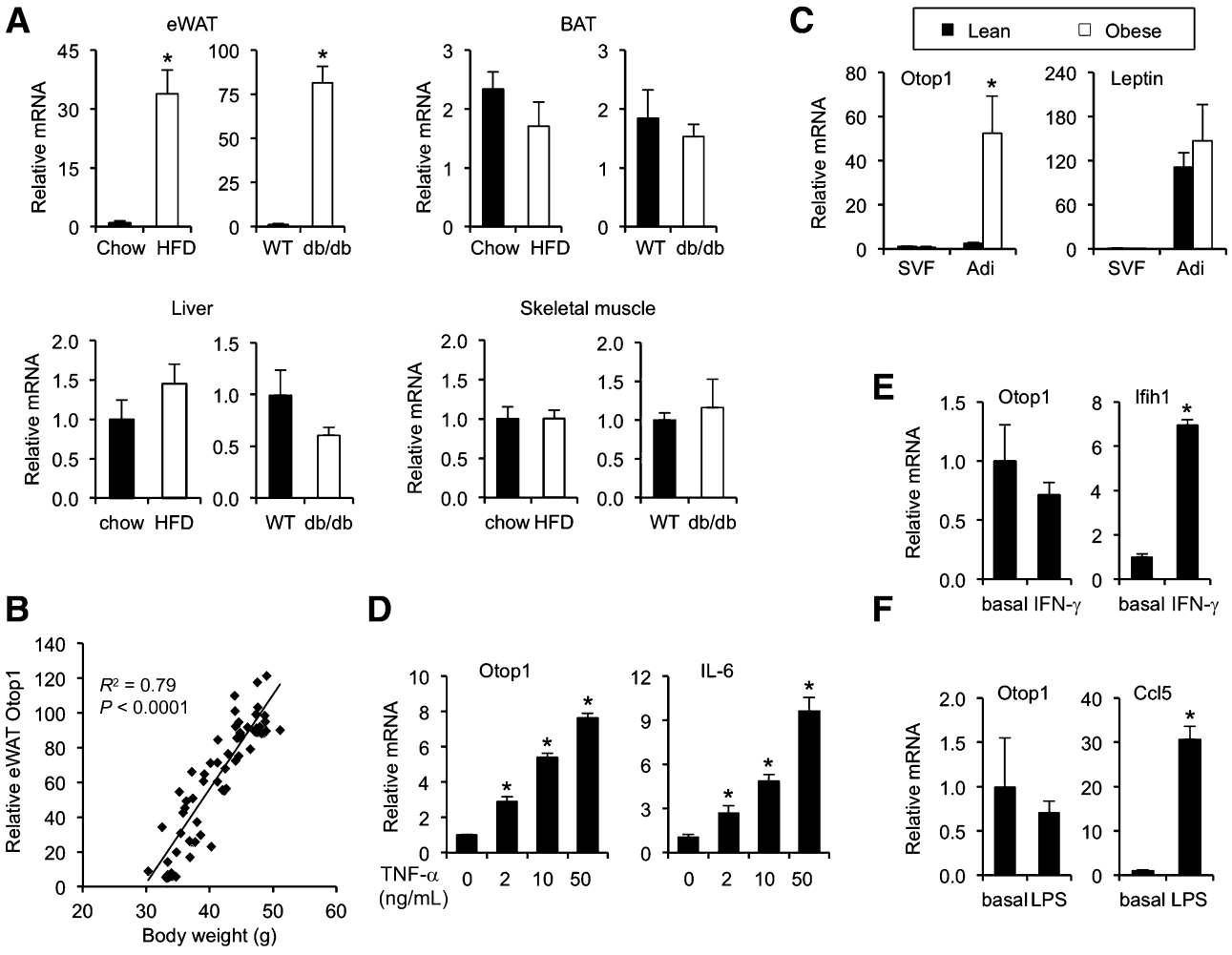

Figure 1—*Otop1* is induced in obese WAT in response to proinflammatory cytokine signaling. (*A*) qPCR analysis of Otop1 expression in tissues from WT mice fed chow (n = 5) or HFD (n = 6) for 3 months (*left*) and from a separate group of WT (n = 4) and db/db mice (n = 4). Data represent mean ± SEM. *P < 0.01, obese vs. lean. (*B*) Correlation of eWAT *Otop1* expression with body weight. Relative *Otop1* mRNA levels were plotted against respective body weight. (*C*) qPCR analysis of SVF and mature adipocyte fractions isolated from eWAT from mice fed chow (n = 3) or HFD (n = 3). Data represent mean ± SEM. *P < 0.01, obese vs. lean. (*D*) qPCR analysis of 3T3-L1 adipocytes treated with indicated concentrations of TNF-α for 6 h. qPCR analysis of 3T3-L1 adipocytes treated with IFN-γ (*E*) or LPS (*F*) for 6 h. Data in *D*–*F* represent mean ± SD from one representative study performed in triplicate wells. *P < 0.01, vs. saline. Adi, adipocyte.

Immunoblotting Analyses

Tissues were homogenized in a lysis buffer containing 50 mmol/L Tris (pH 7.5), 150 mmol/L NaCl, 5 mmol/L NaF, 25 mmol/L β-glycerolphosphate, 1 mmol/L sodium orthovanadate, 10% glycerol, 1% tritonX-100, 1 mmol/L dithiothreitol, and freshly added protease inhibitors. Immunoblotting experiments were performed using specific antibodies and visualized on film using horseradish peroxidase–conjugated secondary antibodies (Sigma and Cell Signaling) and Western Chemiluminescent HRP Substrate (Millipore). Phospho-STAT1 (Y701), phospho-STAT3 (Y705), phospho-STAT5 (Y694), STAT1, STAT3, STAT5, phospho-TBK1 (S172), TBK1, NFκB-p65, phospho-NFκB-p105 (Ser933), NFκB-p105, phospho-AKT (Ser473), phospho-AKT (T308), and AKT antibody were purchased from Cell Signaling Technology. Antibodies against PPAR-γ (Santa Cruz Biotechnology), HA (sc-66181), Flag (Sigma), and tubulin (Sigma) were used.

Affinity Purification of Otop1 Protein Complex

Total cell lysates were prepared from mature brown adipocytes stably expressing murine stem cell virus-vector or murine stem cell virus-Flag-HA-Otop1. Sequential steps of affinity purification was performed using anti-HA (Roche) and anti-Flag (Sigma) affinity matrix followed by eluting with 200 μg/mL HA and Flag peptides, respectively. Eluted protein complex was analyzed by SDS-PAGE. Following colloidal blue staining, individual bands were excised for protein identification by mass spectrometry.

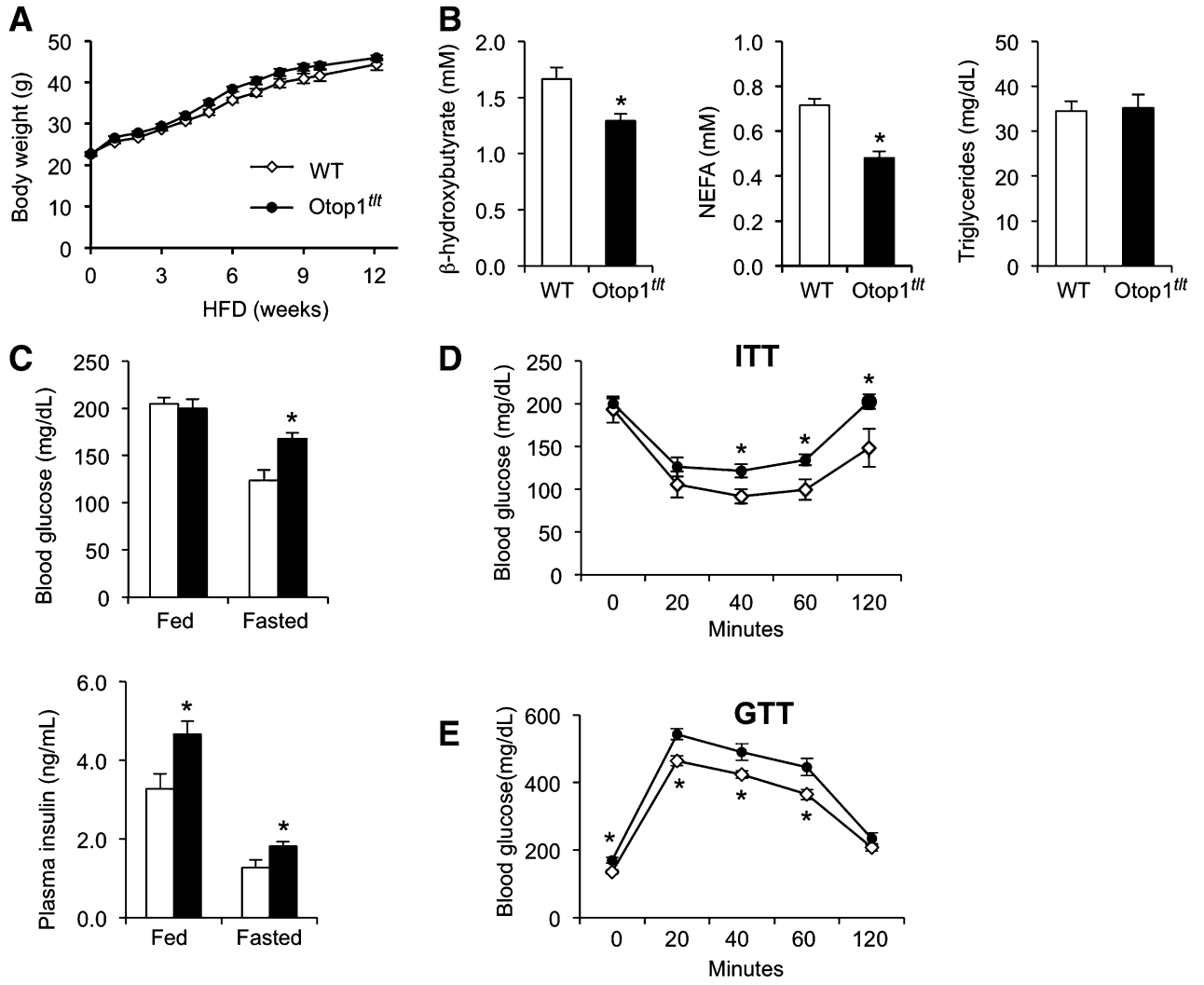

Figure 2—Otop1^{tlt} mutant mice develop more severe HFD-induced insulin resistance. (*A*) Body weight of WT (open diamond; n = 8) and Otop1^{tlt} mice (filled circle; n = 8) during HFD feeding. (*B*) Plasma concentrations of β-hydroxybutyrate, nonesterified fatty acids, and triglycerides after overnight fasting. (*C*) Plasma glucose and insulin levels under fed and fasted conditions. (*D*) Insulin tolerance test in WT (n = 6) and Otop1^{tlt} (n = 7) mice in HFD-fed mice. (*E*) Glucose tolerance test in WT (n = 8) and Otop1^{tlt} mice (n = 8) 9 weeks after HFD feeding. Data represent mean ± SEM. *P < 0.05, Otop1^{tlt} vs. WT. NEFA, nonesterified fatty acids.

Fluorescence-Activated Cell Sorter Analysis

Adipose tissue fractionation, flow cytometry analysis, and whole-mount immunofluorescence staining were performed as previously described (15,16). Blood leukocytes and stromal vascular cells were incubated in Fc Block (rat anti-mouse CD16/32; eBioscience) for 10 min and then stained with CD45-e450, CD11b-APC-Cy7, CD11c-PE-Cy7, CD301-APC, and F4/80-PE (eBioscience) or appropriate isotype controls for 30 min. Labeled cells were then washed twice with fluorescence-activated cell sorter buffer followed by fixation in 1% paraformaldehyde in PBS. Cells were analyzed on FACSCanto II Flow Cytometer (BD Biosciences) using FlowJo software (version 9.6; Treestar). For whole-mount immunostaining, adipose tissue samples were fixed with 1% paraformaldehyde and stained with anti-caveolin and anti-Mac2 antibodies in PBS-T/BSA. Samples were imaged on an inverted confocal microscope using FluoView software (Olympus).

Statistics

Data were analyzed using two-tailed Student *t* test for independent groups. A *P* value of less than 0.05 was considered statistically significant.

RESULTS

Otop1 Is Induced in Obese WAT in Response to Proinflammatory Signaling

Adipose tissue inflammation is emerging as a pathogenic link between obesity and metabolic disorders. The sustained chronic inflammation is associated with a phenotypic switch of resident immune cells from anti-inflammatory to proinflammatory subtypes in adipose tissues (15,17). Whether obesity also activates adaptive mechanisms to counteract inflammation caused by chronic overnutrition remains largely unexplored. *Otop1* mRNA expression is present in BAT but nearly undetectable in eWAT from lean mice. Interestingly, *Otop1* mRNA level was markedly increased in eWAT following

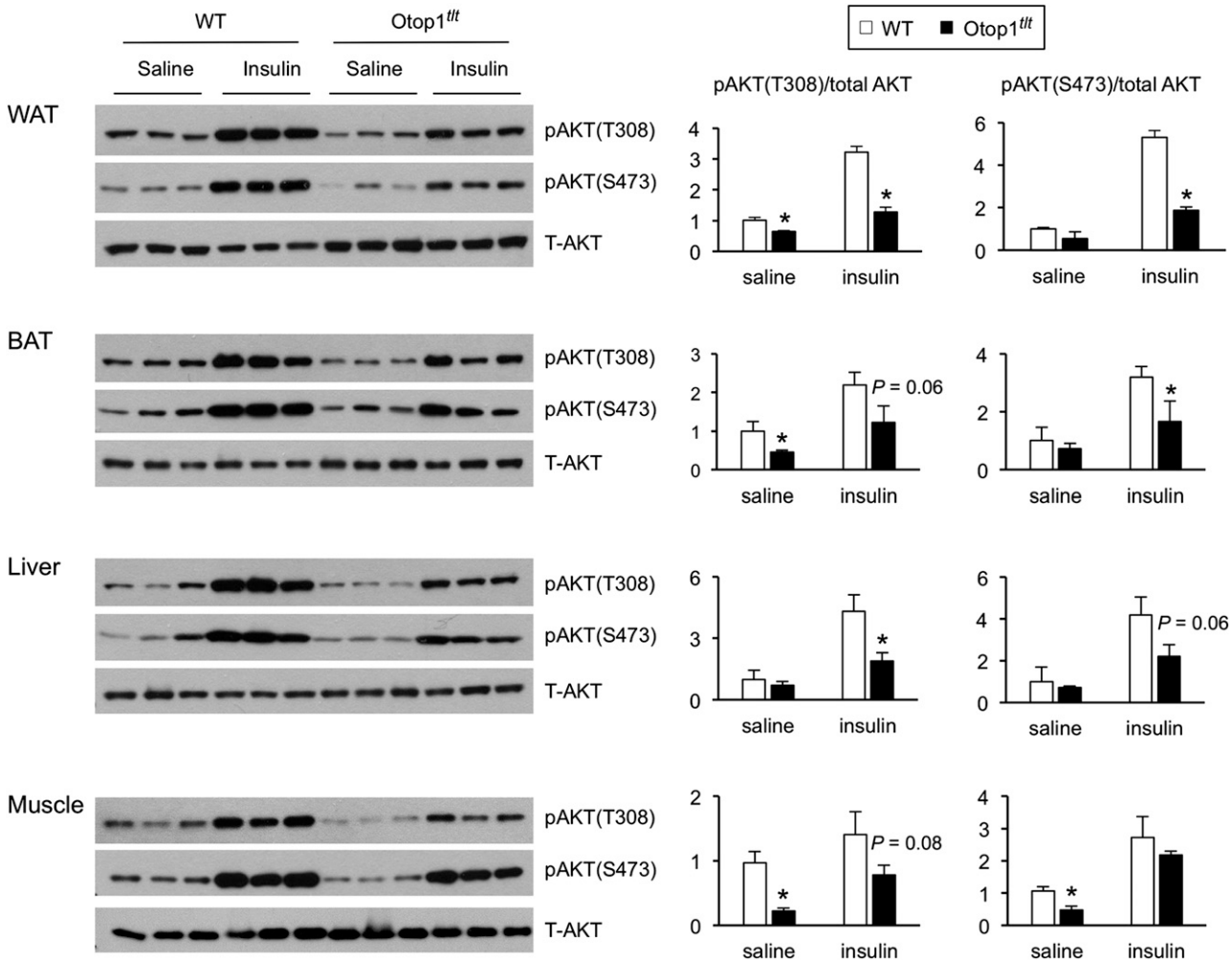

Figure 3—Impaired insulin-stimulated AKT phosphorylation in Otop1^{tlt} mouse tissues. Eight weeks after HFD feeding, tissues were harvested from WT and Otop1^{tlt} mice 10 min after a single intravenous injection of saline or insulin. Immunoblots of total tissue lysates (*left*). Quantitation of phosphorylated AKT was performed following normalization to total AKT levels (*right*). *$P < 0.05$, Otop1^{tlt} vs. WT.

HFD-induced obesity (Fig. 1*A*). Compared with WT, *Otop1* mRNA expression was increased by approximately 80-fold in eWAT from leptin receptor deficient (db/db) mice. Similar increase in *Otop1* expression was also observed in inguinal fat from obese mice (data not shown). In contrast, *Otop1* mRNA levels in BAT remained similar between lean and obese mice (Fig. 1*A*). We did not detect changes in *Otop1* mRNA expression by HFD in other tissues, including skeletal muscle and liver. To determine whether Otop1 expression in eWAT correlates with the severity of obesity, we fed a cohort of C57BL/6J male mice with HFD for 10 weeks to induce obesity. Mice fed HFD gained variable body weight and exhibited different degrees of obesity and insulin resistance. Gene expression analysis in this cohort indicated that eWAT *Otop1* expression was strikingly correlated with body weight of individual mice (Fig. 1*B*). This increase in *Otop1* expression in obese eWAT was due to its induction in mature adipocytes, but not other cell types in the stromal vascular fraction (SVF) (Fig. 1*C*). Expression of leptin was included as markers for mature adipocytes.

Obesity-associated chronic inflammation is characterized by augmented production of proinflammatory cytokines in adipose tissues, such as TNF-α, IFN-γ, IL-1β, and IL-6 (1,20,40). To determine whether Otop1 induction is triggered by proinflammatory cytokines, we treated differentiated 3T3-L1 adipocytes with TNF-α, IFN-γ, or LPS and examined gene expression using qPCR. Compared with control treatments, mRNA expression of *Otop1* and *IL-6*, the latter being a known target gene of TNF-α, was induced by TNF-α in a dose-dependent manner (Fig. 1*D*). In contrast, while IFN-γ and LPS induced the expression of their respective target genes (*Ifih1* and *Ccl5*) in 3T3-L1 adipocytes, these treatments had modest effects on *Otop1* mRNA expression (Fig. 1*E* and *F*). These results suggest that obesity-associated

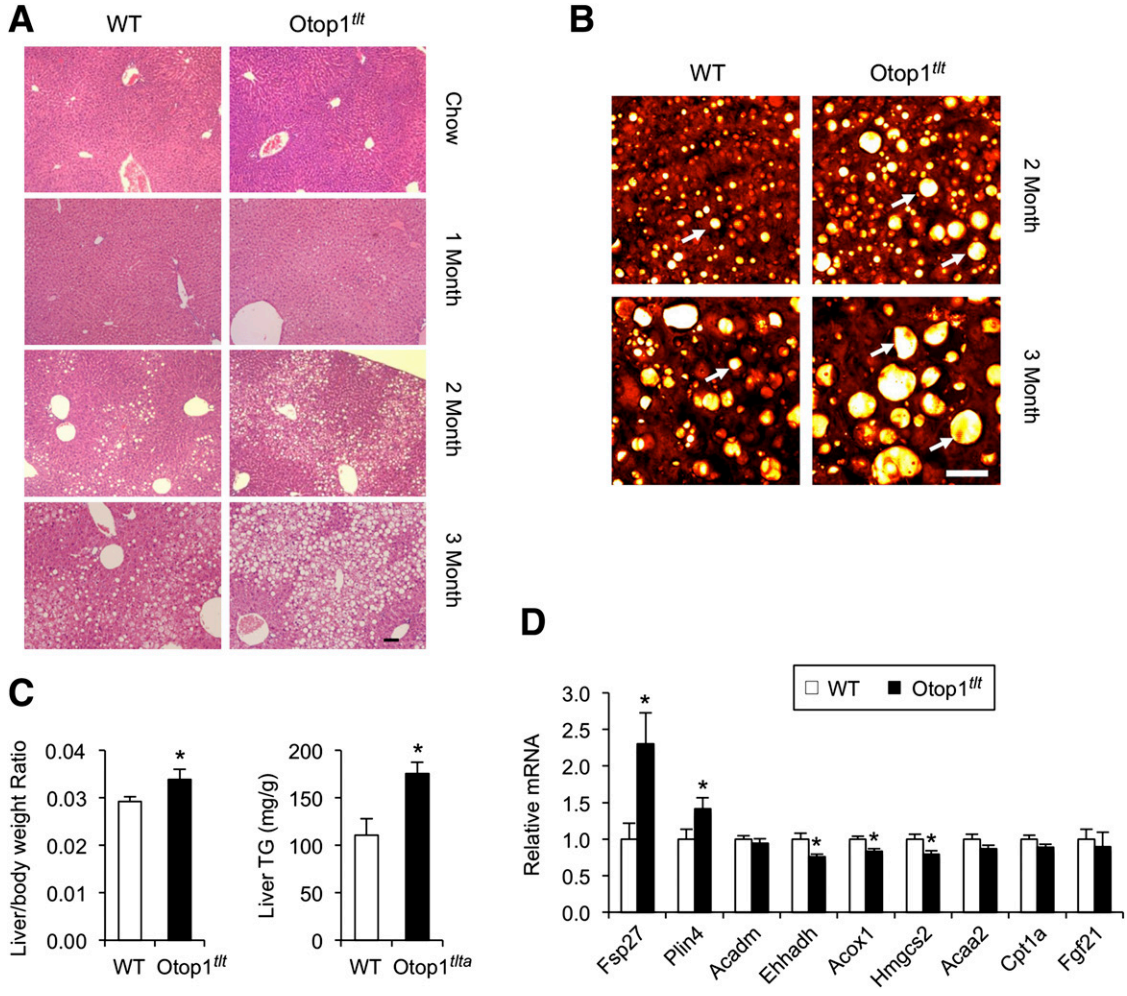

Figure 4—Otop1^{tlt} mutant mice develop more severe diet-induced hepatic steatosis. (*A*) H&E staining of liver sections in WT and Otop1^{tlt} mice fed chow or HFD for different periods of time (scale bar = 100 μm). (*B*) Stimulated Raman scattering imaging of liver sections. Arrows indicate lipid droplets (scale bar = 25 μm). (*C*) Liver/body weight ratio and liver triglyceride content in WT (open; n = 8) and Otop1^{tlt} (filled; n = 8) mice after 3 months of HFD feeding. (*D*) qPCR analysis of hepatic gene expression in WT and Otop1^{tlt} mice. Data in *C* and *D* represent mean ± SEM. *P < 0.05, Otop1^{tlt} vs. WT. TG, triglyceride.

induction of *Otop1* in WAT is likely a direct consequence of heightened adipose tissue inflammation.

Otop1 Mutant Mice Develop More Severe Diet-Induced Metabolic Disorders

While the deleterious effects of innate immune activation have been well established, whether obesity engages an adaptive response to counteract inflammation in adipose tissues has not been elucidated. We next sought to assess the significance of Otop1 in adipose tissue homeostasis, particularly in the context of obesity. WT and Otop1^{tlt} mutant mice gained similar body weight after 12 weeks of HFD feeding (Fig. 2*A*). Plasma concentrations of non-esterified fatty acids and β-hydroxybutyrate, but not triglycerides, were lower in Otop1^{tlt} mutant mice (Fig. 2*B*). Despite a lack of difference in body weight gain, fasting blood glucose and insulin levels were significantly elevated in the mutant mice (Fig. 2*C*). While blood glucose levels were similar under fed conditions, plasma insulin concentration was elevated in Otop1^{tlt} mutant mice. Further, insulin and glucose tolerance tests indicated that mutant mice developed more severe insulin resistance (Fig. 2*D* and *E*), suggesting that Otop1 is required for maintaining insulin sensitivity in diet-induced obesity. In support of this, basal levels of phosphor-AKT were also reduced in adipose tissues and skeletal muscle. Importantly, insulin-stimulated AKT phosphorylation was markedly blunted in several tissues from HFD-fed Otop1^{tlt} mutant mice, including WAT, BAT, liver, and skeletal muscle (Fig. 3). We conclude from these studies that obesity-induced expression of Otop1 in WAT may serve a beneficial role in maintaining metabolic homeostasis in the state of chronic overnutrition.

We performed hematoxylin-eosin (H&E) staining on liver sections from mice fed standard chow or HFD for different periods of time and found that Otop1^{tlt} mice developed

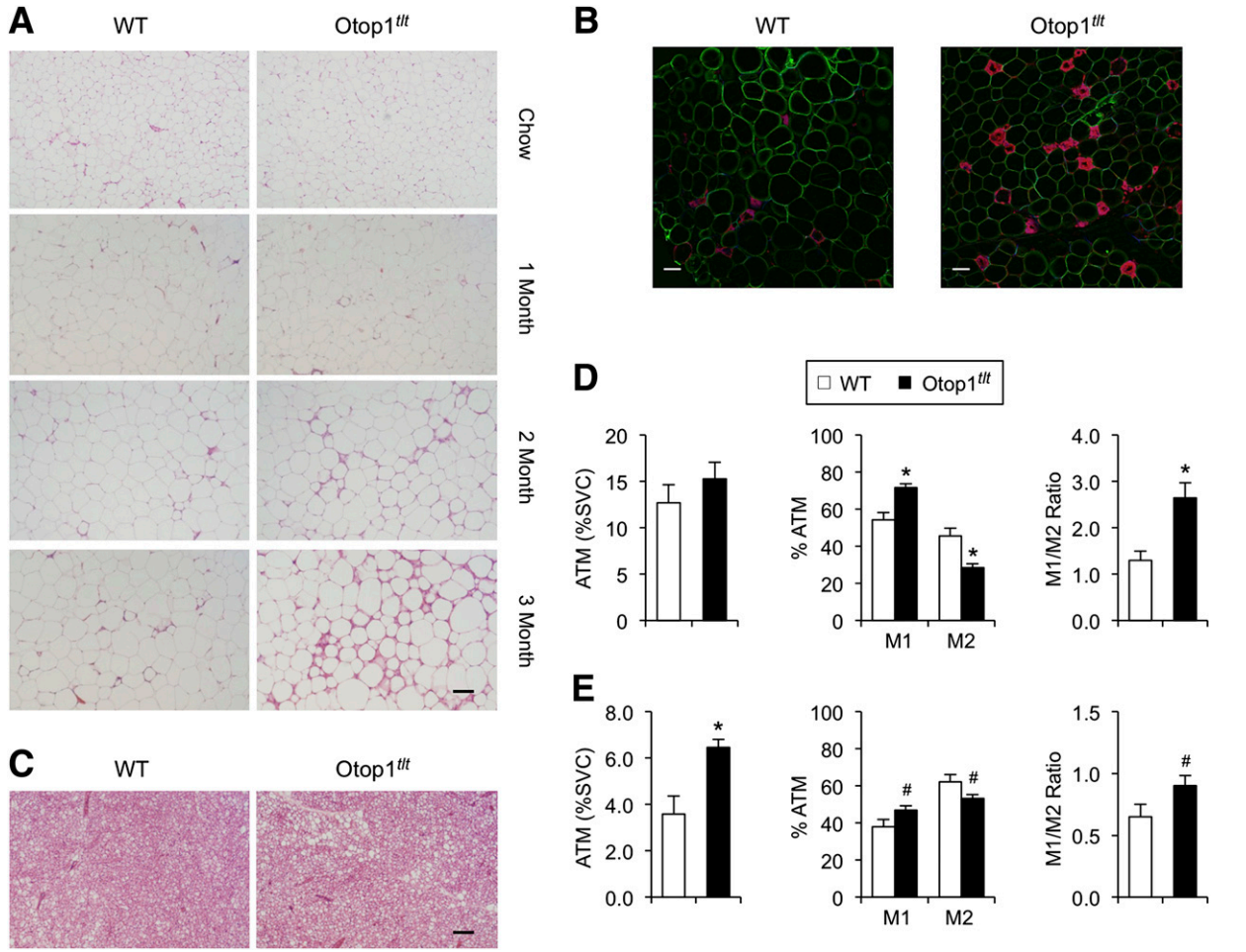

Figure 5—Otop1 mutant mice have exacerbated adipose tissue inflammation following HFD feeding. (*A*) H&E staining of eWAT from WT and Otop1^{tlt} mice fed chow or HFD for different periods of time. Scale bar indicates 100 μm. (*B*) Confocal images of eWAT following whole-mount immunofluorescence staining using caveolin (green) and Mac2 (red) antibodies (scale bar = 50 μm). (*C*) H&E staining of BAT from WT and Otop1^{tlt} mice fed with HFD for 3 months. (*D*) Flow cytometry analyses of adipose tissue macrophages in SVF of eWAT from HFD-fed WT (n = 8) and Otop1^{tlt} (n = 7) mice. (*E*) Flow cytometry analyses of adipose tissue macrophage in iWAT from mice in *D*. Data in *D* and *E* represent mean ± SEM. *P < 0.05, #P < 0.1, Otop1^{tlt} vs. WT. ATM, adipose tissue macrophage.

more severe hepatic steatosis after 2 months on HFD (Fig. 4*A*). These histological findings were confirmed by stimulated Raman scattering microscopy, a label-free imaging method that detects cellular lipids by measuring molecular vibrations of fatty-acyl chains (41,42). As shown in Fig. 4*B*, pericentral hepatocytes from Otop1^{tlt} mutant mice had larger lipid droplets compared with control following 2 and 3 months of HFD feeding. Measurements of liver triglyceride content after 3 months of HFD feeding revealed that Otop1^{tlt} mice had ~58% higher hepatic triglyceride content than WT controls (Fig. 4*C*). In addition, liver/body weight ratio was significantly higher in the mutant mice. Gene expression analysis indicated that mRNA levels of *Fsp27* and *Plin4*, two lipid droplet proteins, were significantly elevated in Otop1^{tlt} mutant livers (Fig. 4*D*). The expression of peroxisomal enoyl-CoA hydratase (*Ehhadh*) and HMG-CoA synthase 2 (*Hmgcs2*), genes involved lipid metabolism, but not fibroblast growth factor 21 (*Fgf21*), was lower in mutant livers. Because *Otop1* expression was nearly undetectable in the liver in lean and obese mice, the exacerbation of hepatic steatosis in mutant mice is most likely secondary to altered adipose tissue metabolism and function.

Otop1 Mutant Mice Exhibit More Severe Adipose Tissue Inflammation Following HFD Feeding

As described above, Otop1 expression was elevated in mouse WAT in obesity and was induced in response to TNF-α treatments in cultured adipocytes (Fig. 1). To our surprise, Otop1 mutant mice showed exacerbated diet-induced insulin resistance and hepatic steatosis. These findings suggest a plausible mechanism where Otop1 contributes to metabolic homeostasis by counteracting obesity-induced adipose tissue inflammation. In support of this, we found that Otop1^{tlt} mutant mice developed progressively more severe adipose tissue inflammation and increased macrophage infiltration as revealed by H&E and whole-mount immunofluorescence staining (Fig. 5*A* and *B*). Compared with WT, the presence of crown-like structures, characteristic of inflamed adipose tissues in obesity, was more pronounced in Otop1^{tlt} mutant eWAT. In contrast, the histological appearance of BATs was similar between the two groups (Fig. 5*C*). We next analyzed the characteristics of adipose tissue macrophages using flow cytometry with specific cell surface markers. Compared with WT, Otop1^{tlt} mutant eWAT had higher proportion of CD301^{-}CD11c^{+} classically polarized (M1) macrophages, whereas alternatively activated (M2) macrophages (CD301^{+}CD11c^{-}) were significantly lower (Fig. 5*D*). Consequently, the M1/M2 ratio was significantly increased in Otop1^{tlt} mutant eWAT. Similar changes in M1/M2 macrophages were also observed in inguinal WAT (iWAT) from Otop1^{tlt} mice (Fig. 5*E*), though the differences only achieved borderline significance.

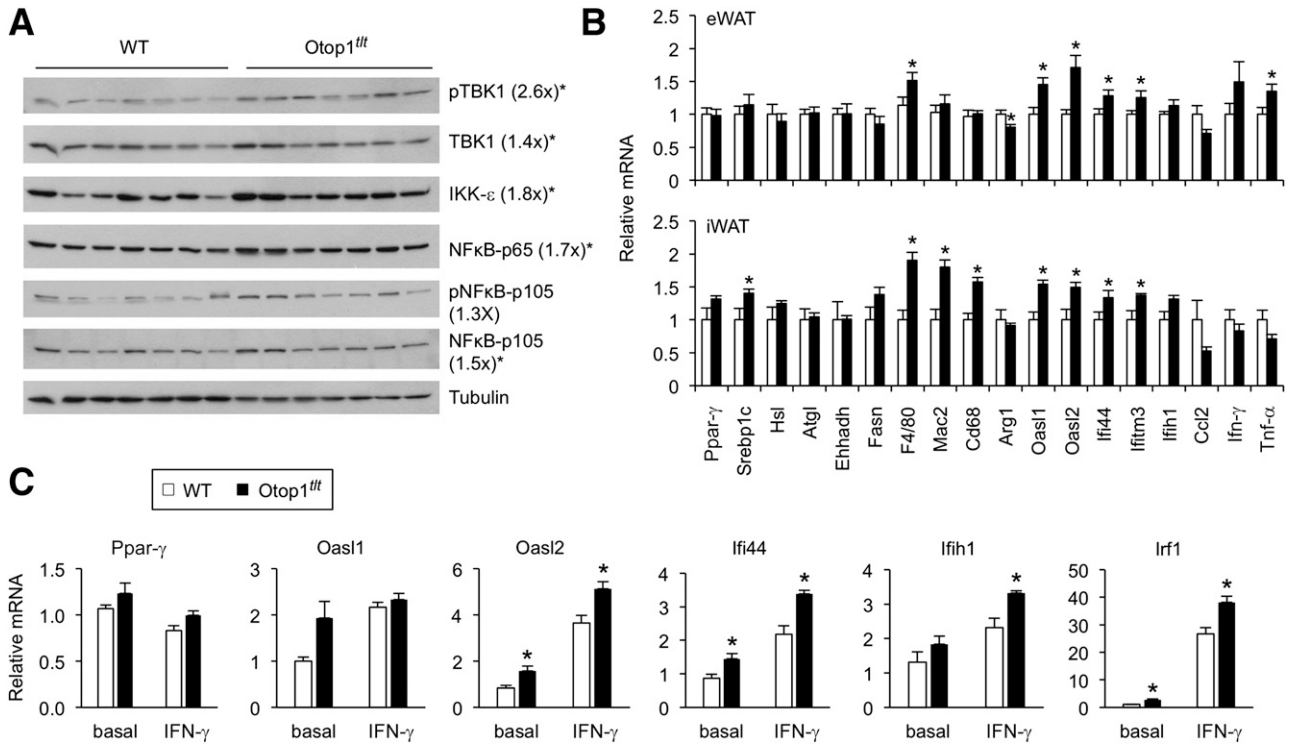

Figure 6—Otop1 negatively regulates WAT inflammation and IFN-γ response. (*A*) Immunoblots of inflammation markers in total eWAT lysates from HFD-fed mice. Fold change in Otop1^{tlt} samples was quantitated following normalization to tubulin. *$P < 0.05$, Otop1^{tlt} vs. WT. (*B*) qPCR analysis of eWAT and iWAT gene expression in HFD-fed WT ($n = 8$) and Otop1^{tlt} ($n = 8$) mice for 3 months. Data represent mean ± SEM. *$P < 0.05$, Otop1^{tlt} vs. WT. (*C*) qPCR analysis of epididymal fat explants from WT and Otop1^{tlt} mutant mice without or with IFN-γ stimulation. Data represent mean ± SD from triplicate wells. *$P < 0.05$, Otop1^{tlt} vs. WT.

We next performed immunoblotting and qPCR analyses to examine molecular changes in adipose tissues from HFD-fed control and Otop1 mutant mice. Immunoblotting studies revealed that protein levels of IKK-ε, a target of NFκB recently implicated in obesity-induced adipose tissue inflammation (23,43), were increased in Otop1 mutant eWAT (Fig. 6*A*). Consistently, NFκB-p105, phospho-NFκB-p105, and NFκB-p65 protein levels were elevated in Otop1^{tlt} mutant eWAT. Total TBK1 and phospho-TBK1 protein levels were also higher in Otop1^{tlt} mutant eWAT. mRNA expression of many metabolic genes was similar between two groups, including *PPAR-γ* and *Srebp1c*, key regulators of adipocyte gene expression, hormone-sensitive lipase (*Hsl*), adipose triglyceride lipase (*Atgl*), and *Ehhadh* (Fig. 6*B*). Consistent with changes in macrophage subtypes, we found that mRNA expression of macrophage marker *F4/80* was elevated, whereas the expression of arginase 1 (*Arg1*), a marker for M2 macrophages, was significantly lower in mutant eWAT. The expression levels of *Mac2* and *Cd68* were also elevated in Otop1 mutant iWAT. In contrast, the expression of *TNF-α* and many IFN-γ target genes, including 2′-5′ oligoadenylate synthetase-like-1 (*Oasl1*), *Oasl2*, IFN-induced protein 44 (*Ifi44*), and IFN-induced transmembrane protein 3 (*Ifitm3*), was significantly higher in Otop1^{tlt} eWAT than control. Similar induction of macrophage markers and IFN-γ target genes was observed in Otop1^{tlt} mutant mouse iWAT (Fig. 6*B*). Because IFN-γ expression remained largely unaltered, the induction of its target genes in mutant WAT is likely due to augmented IFN-γ signaling in Otop1^{tlt} mutant adipocytes. To directly test this, we treated epididymal fat explants from HFD-fed WT and Otop1^{tlt} mutant mice with IFN-γ and examined target gene responses. The induction of several IFN-γ target genes, including *Oasl2*, *Ifi44*, *Ifih1*, and IFN regulatory factor-1 (*Irf1*), was significantly higher in Otop1^{tlt} mutant fat explants than control in response to IFN-γ stimulation (Fig. 6*C*). Together, these results suggest that Otop1 induction in obese WAT is likely an adaptive homeostatic response that exerts a protective role by counteracting obesity-induced adipose inflammation.

Otop1 Interacts With STAT1 and Attenuates IFN-γ Signaling in Adipocytes

To explore the molecular mechanisms by which Otop1 modulates IFN-γ signaling, we ectopically expressed

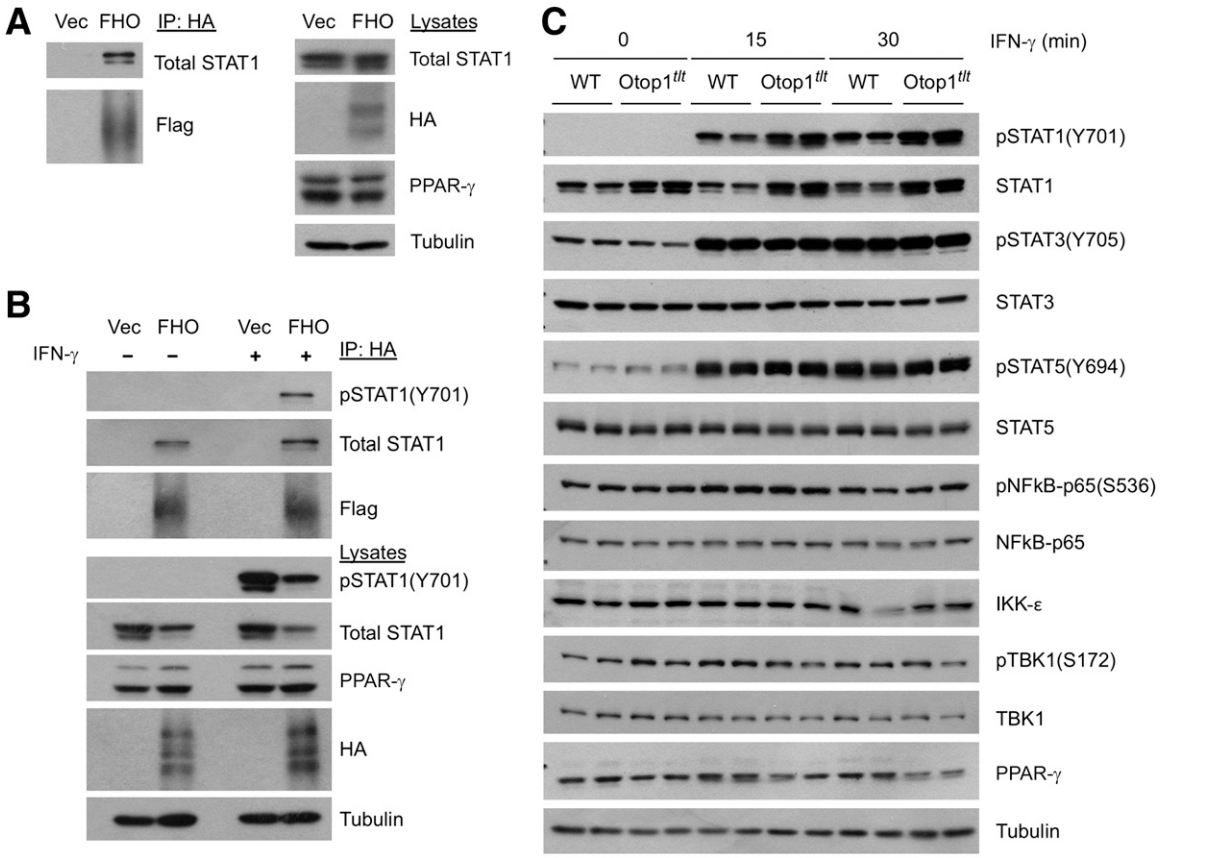

Figure 7—Otop1 physically interacts with STAT1 and regulates IFN-γ response in adipocytes. Immunoblots of total cell lysates and immunoprecipitated (IP) proteins (anti-HA) from differentiated 3T3-L1 adipocytes (*A*) or brown adipocytes (*B*) stably expressing vector or Flag-HA-tagged Otop1 and treated with vehicle or IFN-γ. (*C*) Immunoblots of total cell lysates from brown adipocytes stably expressing vector or Otop1 treated with saline (-) or IFN-γ (+) for indicated time. Vec, vector; FHO, Flag-HA-tagged Otop1.

Flag-HA-tagged Otop1 in 3T3-L1 and immortalized brown preadipocytes and performed immunoaffinity purification of the Otop1 protein complexes. Mass spectrometry and immunoblotting analyses indicated that Otop1 physically interacted with STAT1 (Fig. 7*A* and *B*), a transcription factor that plays a critical role in IFN-γ signaling (28). The interaction between Otop1 and STAT1 appears to be independent of STAT1 phosphorylation (Fig. 7*B*). To determine whether the exacerbation of adipose tissue inflammation in Otop1 mutant mice results from cell-autonomous effects of Otop1 on inflammatory signaling, we first examined the response of WT and Otop1 mutant adipocytes to IFN-γ treatments. Because brown adipocytes express endogenous Otop1, we immortalized brown preadipocytes from WT and Otop1 mutant neonates and performed studies following adipocyte differentiation. As expected, IFN-γ treatments strongly induced tyrosine phosphorylation of STAT1, STAT3, and STAT5 but only had modest effects on the NFκB and IKK-ε/TBK1 pathways (Fig. 7*C*). Total and phosphorylated STAT3 and STAT5 proteins were comparable between WT and Otop1 mutant adipocytes. In contrast, total STAT1 protein levels were elevated in mutant adipocytes, resulting in more robust tyrosine phosphorylation in response to IFN-γ treatments.

We performed microarray studies to identify downstream pathways that were affected by Otop1 mutation. Consistent with the eWAT gene expression profile, the expression of a large number of IFN-γ target genes, including *Oasl1*, *Oasl2*, *Ifi44*, *Ifitm3*, and *Ifih1*, was significantly elevated in Otop1 mutant adipocytes compared with control (Fig. 8*A*). In response to IFN-γ treatments, mRNA expression of these target genes was induced to higher levels in Otop1 mutant adipocytes compared with WT control (Fig. 8*B*). These results strongly suggest that Otop1 attenuates IFN-γ signaling in adipocytes through its physical interaction with STAT1 (Fig. 8*C*).

We further assessed whether ectopic overexpression of Otop1 attenuates the IFN-γ/STAT1 signaling pathway in adipocytes. We treated differentiated brown adipocytes expressing vector or Otop1 with IFN-γ and examined STAT1 protein levels and phosphorylation. Compared with vector, Otop1 overexpression significantly decreased total STAT1 protein levels and phosphorylated STAT1 following IFN-γ stimulation (Fig. 9*A*). In contrast, protein levels of STAT3, NFκB, and IKK-ε/TBK1 remained largely unaltered by Otop1. Basal STAT5 phosphorylation is slightly lower in adipocytes overexpressing Otop1, yet the differences disappeared after IFN-γ treatment. Consistent with decreased STAT1 levels, basal expression of IFN-γ targets such as *Ifi44*, *Oasl1*, *Oasl2*, and *Ifih1* was reduced by retroviral-mediated overexpression of Otop1 (Fig. 9*B*). Further, the induction of these genes in response to IFN-γ was also significantly dampened in Otop1-overexpressing adipocytes. Taken together, we conclude that Otop1 negatively regulates IFN-γ signaling in adipocytes and may

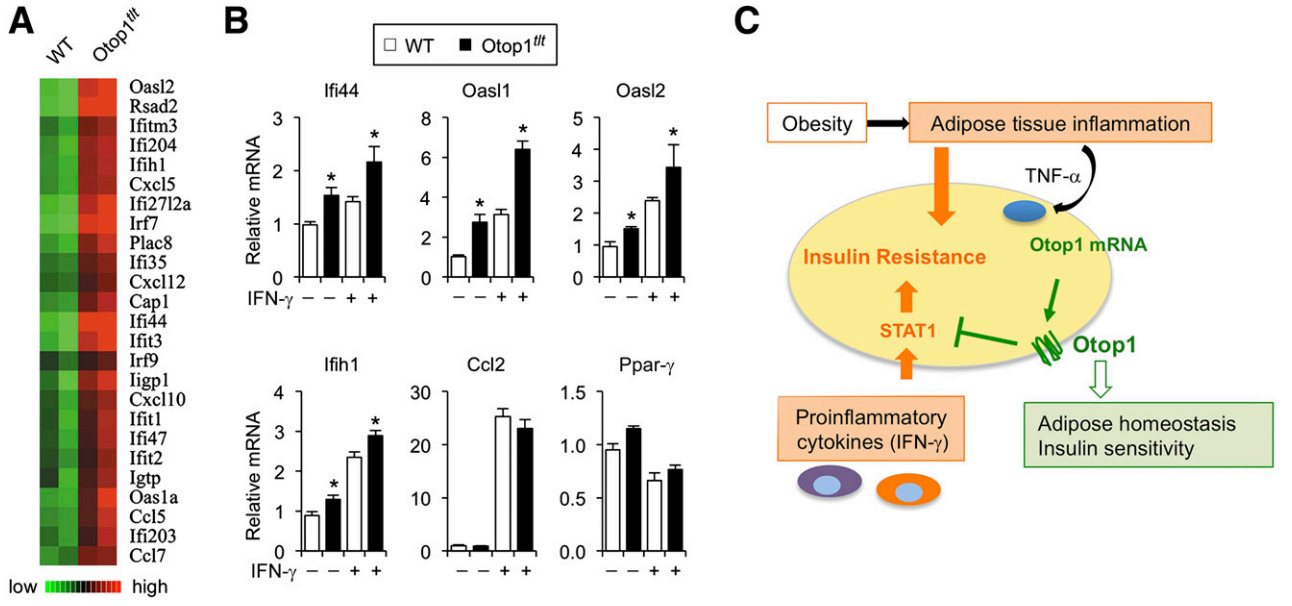

Figure 8—IFN-γ signaling is augmented in Otop1^{tlt} mutant adipocytes. (*A*) Clustering analysis of IFN-γ target genes in differentiated WT and Otop1^{tlt} brown adipocytes. (*B*) qPCR analysis of gene expression in differentiated adipocytes treated with saline (-) or 10 ng/mL IFN-γ (+) for 4 h. Data represent mean ± SD from triplicate wells. *$P < 0.05$, Otop1^{tlt} vs. WT. (*C*) Model depicting the role of Otop1 in counteracting obesity-associated inflammation in adipocytes. Otop1 expression is induced by TNF-α in white fat during obesity. The induction of Otop1 serves to attenuate proinflammatory cytokine signaling in adipocytes and maintain adipose tissue function and systemic metabolic homeostasis.

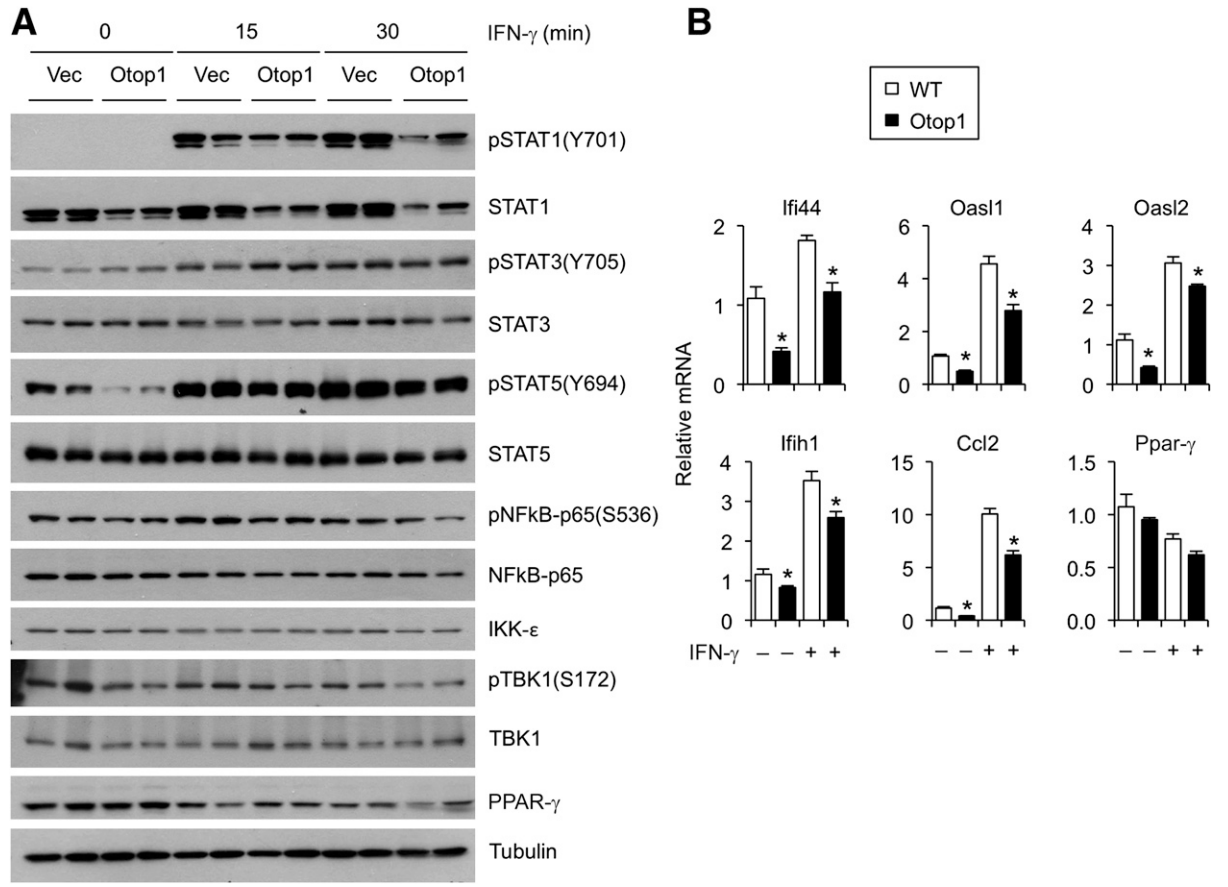

Figure 9—Otop1 attenuates IFN-γ signaling in adipocytes. (*A*) Immunoblots of total cell lysates from brown adipocytes stably expressing vector or Otop1 treated with saline or IFN-γ for 15 or 30 min. (*B*) qPCR analysis of gene expression in differentiated brown adipocytes stably expressing vector or Otop1 treated with saline (-) or 10 ng/mL IFN-γ (+) for 4 h. Data represent mean ± SD from triplicate wells. *$P <$ 0.05, Otop1 vs. vector. Vec, vector.

serve to counteract chronic proinflammatory immune response in obese adipose tissues.

DISCUSSION

The pathogenic role of chronic inflammation in the development of obesity-associated metabolic disease has been well established. Attenuation of inflammatory signaling generally resulted in improved metabolic profiles in rodent models of obesity. While counterinflammation has been proposed as a key aspect of homeostatic regulation (44), the molecular components of this negative feedback arm remain elusive. In this study, we identified Otop1 as an obesity-induced target of cytokine signaling in WAT. Otop1 mutant mice develop more severe diet-induced insulin resistance and hepatic steatosis that are accompanied by augmented adipose tissue inflammation. Otop1 interacts with Stat1 and attenuates IFN-γ signaling in adipocytes in a cell-autonomous manner. Together, these studies illustrate a novel pathway that counteracts obesity-associated chronic inflammation and preserves metabolic homeostasis in obesity (Fig. 8*C*).

A remarkable aspect of Otop1 expression in WAT is that it is highly induced during obesity. Thus mRNA levels of Otop1 in WAT correlate tightly with the degree of HFD-induced obesity. Elevated expression of Otop1 was also observed in white fat depots from db/db mice. While it is possible that the induction of Otop1 expression in obese adipose tissues may result from changes in cell populations in WAT, gene expression analyses in fractionated adipocytes and stromal vascular cells indicated that Otop1 induction occurred exclusively in adipocytes. Otop1 mRNA was nearly undetectable in the SVF. The stimuli that drive obesity-associated induction of Otop1 in adipocytes may be multifaceted in nature. In cultured 3T3-L1 adipocytes, the proinflammatory cytokine TNF-α, but not IFN-γ and LPS, strongly induced Otop1 expression in a dose-dependent manner, suggesting that Otop1 is likely a target downstream of a subset of proinflammatory signals.

Otop1 mutant mice developed diet-induced obesity at similar pace compared with controls, suggesting that Otop1 does not play a major role in the regulation of whole body energy balance. A surprise here is that the mutant mice developed more severe insulin resistance and hepatic steatosis. Because Otop1 expression was not detected in the liver in lean and obese mice, the

exacerbation of liver fat accumulation in HFD-fed Otop1 mutant mice was most likely secondary to the metabolic perturbations that occurred in mutant adipose tissues. In support of this, we found that the formation of crown-like structures, which are indicative of adipocyte death and inflammatory response, was accelerated in Otop1 mutant adipose tissue. The increase in crown-like structures was accompanied by a shift in macrophage polarization toward a proinflammatory subtype. Accordingly, mRNA and protein markers of inflammatory signaling were also elevated in Otop1 mutant eWAT following HFD feeding. These observations are consistent with a critical role for Otop1 in attenuating obesity-associated inflammation. This mechanism is apparently distinct from the counterinflammatory actions of noncanonical IKKs, i.e., IKK-ε and TBK1, which are induced in obesity to sustain chronic inflammation in adipose tissue (23,43). Recent studies have also implicated GPR120 as a sensor for anti-inflammatory fatty acids with insulin-sensitizing effects (45). However, GPR120 appears to act primarily in macrophages. As such, concerted activation of counterinflammation in both adipocytes and immune cells is required for maintaining normal adipose tissue function and metabolic homeostasis.

The mechanisms by which Otop1 exerts its anti-inflammatory effects appear to be mediated, at least in part, by attenuating IFN-γ signaling in adipocytes. IFN-γ is primarily produced by natural killer and T cells and plays an important role in M1 macrophage activation (46). IFN-γ also directly activates its receptors on adipocytes and elicits its effects on cytokine expression and metabolism (29,47). Interestingly, IFN-γ deficient mice have an improved metabolic profile following HFD feeding (30,48), suggesting that excess IFN-γ signaling may have deleterious effects on adipose tissue function and systemic metabolism. The expression of a number of IFN-γ target genes was elevated in Otop1 mutant eWAT. Importantly, the inhibitory effects of Otop1 on IFN-γ target gene expression appears to be cell autonomous, as Otop1 mutant adipocytes have elevated expression of these genes at baseline. In response to IFN-γ treatments, the induction of these genes was further augmented. In contrast, overexpression of Otop1 in adipocytes significantly blunted IFN-γ-induced gene expression. These gain- and loss-of-function studies suggest that exacerbated adipose tissue inflammation in Otop1 mutant mice is likely due to augmented proinflammatory cytokine signaling in adipocytes. At the molecular level, Otop1 physically interacts with STAT1, a downstream transcription factor essential for IFN-γ signaling, and selectively reduces STAT1 protein expression in adipocytes. The biochemical mechanisms underlying the downregulation of STAT1 by Otop1 remain currently unknown.

Previous studies have established the framework for the involvements of chronic inflammation in the pathogenesis of obesity-related adipose tissue dysfunction and metabolic disease. However, surprisingly little is known about potential activation of anti-inflammatory pathways that may counterbalance excess inflammation in the state of overnutrition. Disruption of the proinflammatory signaling cascades via genetic or pharmacological means has been proven effective in mitigating metabolic disease. As such, it is only logical to speculate that a putative component of the anti-inflammatory arm is itself a target of inflammatory signaling and that the deficiency of this counterregulatory arm may worsen obesity-induced metabolic disorders. Thus Otop1 is likely a component of a novel counterinflammatory signaling pathway that maintains adipose immune homeostasis in obesity. Activation of this adaptive pathway may provide metabolic benefits in obesity.

Acknowledgments. The authors are grateful to Q. Yu and W. Lin (Life Sciences Institute, University of Michigan) for technical assistance and members of the laboratory for discussions. The authors thank D. Ornitz (Department of Developmental Biology, Washington University) for sharing Otop1 reagents and X.W. Chen (Life Sciences Institute, University of Michigan) for help with adipocyte studies.

Funding. This work was supported by the National Institutes of Health (DK-077086 and DK-095151 [J.D.L.] and DK-090262 and DK-092873 [C.N.L.]) and a Career Development Award from the American Diabetes Association (J.D.L.). Core services were provided by the Michigan Diabetes Research and Training Center (DK-020572) and the Nutrition Obesity Research Center (DK-089503). S.L. and G.-X.W. were supported by an American Heart Association Scientist Development Grant and a predoctoral fellowship, respectively.

Duality of Interest. No potential conflicts of interest relevant to this article were reported.

Author Contributions. G.-X.W. and J.D.L. conceived the project, designed the experiments, performed studies, analyzed the data, and wrote the manuscript. K.W.C., M.U., C.-R.H., S.L., Z.C., A.E.X., J.-X.C., A.R.S., and C.N.L. performed studies and analyzed the data. J.D.L. is the guarantor of this work and, as such, had full access to all the data in the study and takes responsibility for the integrity of the data and the accuracy of the data analysis.

References

1. Trujillo ME, Scherer PE. Adipose tissue-derived factors: impact on health and disease. Endocr Rev 2006;27:762–778
2. Tontonoz P, Spiegelman BM. Fat and beyond: the diverse biology of PPARgamma. Annu Rev Biochem 2008;77:289–312
3. Cannon B, Nedergaard J. Brown adipose tissue: function and physiological significance. Physiol Rev 2004;84:277–359
4. Lowell BB, Spiegelman BM. Towards a molecular understanding of adaptive thermogenesis. Nature 2000;404:652–660
5. Gregor MF, Hotamisligil GS. Inflammatory mechanisms in obesity. Annu Rev Immunol 2011;29:415–445
6. Lumeng CN, Saltiel AR. Inflammatory links between obesity and metabolic disease. J Clin Invest 2011;121:2111–2117
7. Odegaard JI, Chawla A. Pleiotropic actions of insulin resistance and inflammation in metabolic homeostasis. Science 2013;339:172–177
8. Osborn O, Olefsky JM. The cellular and signaling networks linking the immune system and metabolism in disease. Nat Med 2012;18:363–374
9. Sun S, Ji Y, Kersten S, Qi L. Mechanisms of inflammatory responses in obese adipose tissue. Annu Rev Nutr 2012;32:261–286

10. Goldfine AB, Silver R, Aldhahi W, et al. Use of salsalate to target inflammation in the treatment of insulin resistance and type 2 diabetes. Clin Transl Sci 2008;1:36–43
11. Larsen CM, Faulenbach M, Vaag A, et al. Interleukin-1-receptor antagonist in type 2 diabetes mellitus. N Engl J Med 2007;356:1517–1526
12. Hevener AL, Olefsky JM, Reichart D, et al. Macrophage PPAR gamma is required for normal skeletal muscle and hepatic insulin sensitivity and full antidiabetic effects of thiazolidinediones. J Clin Invest 2007;117:1658–1669
13. Pascual G, Fong AL, Ogawa S, et al. A SUMOylation-dependent pathway mediates transrepression of inflammatory response genes by PPAR-gamma. Nature 2005;437:759–763
14. Aron-Wisnewsky J, Tordjman J, Poitou C, et al. Human adipose tissue macrophages: m1 and m2 cell surface markers in subcutaneous and omental depots and after weight loss. J Clin Endocrinol Metab 2009;94:4619–4623
15. Lumeng CN, Bodzin JL, Saltiel AR. Obesity induces a phenotypic switch in adipose tissue macrophage polarization. J Clin Invest 2007;117:175–184
16. Lumeng CN, Deyoung SM, Bodzin JL, Saltiel AR. Increased inflammatory properties of adipose tissue macrophages recruited during diet-induced obesity. Diabetes 2007;56:16–23
17. Feuerer M, Herrero L, Cipolletta D, et al. Lean, but not obese, fat is enriched for a unique population of regulatory T cells that affect metabolic parameters. Nat Med 2009;15:930–939
18. Nishimura S, Manabe I, Nagasaki M, et al. CD8+ effector T cells contribute to macrophage recruitment and adipose tissue inflammation in obesity. Nat Med 2009;15:914–920
19. Winer S, Chan Y, Paltser G, et al. Normalization of obesity-associated insulin resistance through immunotherapy. Nat Med 2009;15:921–929
20. Hotamisligil GS, Shargill NS, Spiegelman BM. Adipose expression of tumor necrosis factor-alpha: direct role in obesity-linked insulin resistance. Science 1993;259:87–91
21. Arkan MC, Hevener AL, Greten FR, et al. IKK-beta links inflammation to obesity-induced insulin resistance. Nat Med 2005;11:191–198
22. Cai D, Yuan M, Frantz DF, et al. Local and systemic insulin resistance resulting from hepatic activation of IKK-beta and NF-kappaB. Nat Med 2005;11:183–190
23. Chiang SH, Bazuine M, Lumeng CN, et al. The protein kinase IKKepsilon regulates energy balance in obese mice. Cell 2009;138:961–975
24. Hirosumi J, Tuncman G, Chang L, et al. A central role for JNK in obesity and insulin resistance. Nature 2002;420:333–336
25. Stienstra R, Joosten LA, Koenen T, et al. The inflammasome-mediated caspase-1 activation controls adipocyte differentiation and insulin sensitivity. Cell Metab 2010;12:593–605
26. Vandanmagsar B, Youm YH, Ravussin A, et al. The NLRP3 inflammasome instigates obesity-induced inflammation and insulin resistance. Nat Med 2011;17:179–188
27. Waki H, Tontonoz P. Endocrine functions of adipose tissue. Annu Rev Pathol 2007;2:31–56
28. Stark GR, Darnell JE Jr. The JAK-STAT pathway at twenty. Immunity 2012;36:503–514
29. McGillicuddy FC, Chiquoine EH, Hinkle CC, et al. Interferon gamma attenuates insulin signaling, lipid storage, and differentiation in human adipocytes via activation of the JAK/STAT pathway. J Biol Chem 2009;284:31936–31944
30. Rocha VZ, Folco EJ, Sukhova G, et al. Interferon-gamma, a Th1 cytokine, regulates fat inflammation: a role for adaptive immunity in obesity. Circ Res 2008;103:467–476
31. Hughes I, Binkley J, Hurle B, Green ED, Sidow A, Ornitz DM; NISC Comparative Sequencing Program. Identification of the Otopetrin Domain, a conserved domain in vertebrate otopetrins and invertebrate otopetrin-like family members. BMC Evol Biol 2008;8:41
32. Hurle B, Marques-Bonet T, Antonacci F, et al.; NISC Comparative Sequencing Program. Lineage-specific evolution of the vertebrate Otopetrin gene family revealed by comparative genomic analyses. BMC Evol Biol 2011;11:23
33. Hughes I, Saito M, Schlesinger PH, Ornitz DM. Otopetrin 1 activation by purinergic nucleotides regulates intracellular calcium. Proc Natl Acad Sci USA 2007;104:12023–12028
34. Hurle B, Ignatova E, Massironi SM, et al. Non-syndromic vestibular disorder with otoconial agenesis in tilted/mergulhador mice caused by mutations in otopetrin 1. Hum Mol Genet 2003;12:777–789
35. Kim E, Hyrc KL, Speck J, et al. Missense mutations in Otopetrin 1 affect subcellular localization and inhibition of purinergic signaling in vestibular supporting cells. Mol Cell Neurosci 2011;46:655–661
36. Kim E, Hyrc KL, Speck J, et al. Regulation of cellular calcium in vestibular supporting cells by otopetrin 1. J Neurophysiol 2010;104:3439–3450
37. Klein J, Fasshauer M, Ito M, Lowell BB, Benito M, Kahn CR. beta(3)-adrenergic stimulation differentially inhibits insulin signaling and decreases insulin-induced glucose uptake in brown adipocytes. J Biol Chem 1999;274:34795–34802
38. Li S, Liu C, Li N, et al. Genome-wide coactivation analysis of PGC-1alpha identifies BAF60a as a regulator of hepatic lipid metabolism. Cell Metab 2008;8:105–117
39. Molusky MM, Li S, Ma D, Yu L, Lin JD. Ubiquitin-specific protease 2 regulates hepatic gluconeogenesis and diurnal glucose metabolism through 11β-hydroxysteroid dehydrogenase 1. Diabetes 2012;61:1025–1035
40. Rotter V, Nagaev I, Smith U. Interleukin-6 (IL-6) induces insulin resistance in 3T3-L1 adipocytes and is, like IL-8 and tumor necrosis factor-alpha, overexpressed in human fat cells from insulin-resistant subjects. J Biol Chem 2003;278:45777–45784
41. Folick A, Min W, Wang MC. Label-free imaging of lipid dynamics using Coherent Anti-stokes Raman Scattering (CARS) and Stimulated Raman Scattering (SRS) microscopy. Curr Opin Genet Dev 2011;21:585–590
42. Le TT, Yue S, Cheng JX. Shedding new light on lipid biology with coherent anti-Stokes Raman scattering microscopy. J Lipid Res 2010;51:3091–3102
43. Reilly SM, Chiang SH, Decker SJ, et al. An inhibitor of the protein kinases TBK1 and IKK-ε improves obesity-related metabolic dysfunctions in mice. Nat Med 2013;19:313–321
44. Saltiel AR. Insulin resistance in the defense against obesity. Cell Metab 2012;15:798–804
45. Oh DY, Talukdar S, Bae EJ, et al. GPR120 is an omega-3 fatty acid receptor mediating potent anti-inflammatory and insulin-sensitizing effects. Cell 2010;142:687–698
46. Hu X, Ivashkiv LB. Cross-regulation of signaling pathways by interferon-gamma: implications for immune responses and autoimmune diseases. Immunity 2009;31:539–550
47. Wada T, Hoshino M, Kimura Y, et al. Both type I and II IFN induce insulin resistance by inducing different isoforms of SOCS expression in 3T3-L1 adipocytes. Am J Physiol Endocrinol Metab 2011;300:E1112–E1123
48. O'Rourke RW, White AE, Metcalf MD, et al. Systemic inflammation and insulin sensitivity in obese IFN-γ knockout mice. Metabolism 2012;61:1152–1161